

STORAGE RING FREE-ELECTRON LASER SATURATION FOR CHROMATIC AND ACHROMATIC OPTICS *

M. Hosaka, A. Mochihashi, M. Katoh, UVSOR Facility, Institute for Molecular Science, Japan
 Y. Takashima, Graduate School of Engineering, Nagoya University, Japan
 M. Labat, M. E. Couprie CEA/DSM/DRECAM/Service de Photons, Atomes et molecules, France

Abstract

In a Storage Ring Free Electron Laser (FEL), the saturation mechanism results from the so-called “bunch heating” phenomenon. The periodic interaction between the electron bunch and the laser pulse within the cavity is responsible of the enhancement of the energy spread of the bunch correlated with a bunch lengthening. Recently, new electron beam optics aiming at achieving low emittance with distributed dispersive function η revealed a particular interest for the FEL. In the undulator straight section, the FEL interaction for these optics lead also to an increase of the transverse sizes of the beam, and to a significant change of the Touschek lifetime. Experimental results obtained on the Super-ACO and UVSOR-II FELs illustrating the change of saturation process according to the chromatic or achromatic optics are given. They are compared with simulations performed with the LAS model, which has been modified to represent this new saturation process.

INTRODUCTION

On a storage ring Free Electron Laser (FEL), the saturation takes place when the gain reaches the optical cavity losses due to an enhancement of the energy spread σ_γ/γ , the so-called “bunch heating” and its correlated bunch lengthening. Then, due to the synchrotron motion, electrons oscillate longitudinally inside the bunch at a frequency which is proportional to the square root of the momentum compaction factor α [1, 2]. They are then refreshed in a time typically equal to the synchrotron damping time. Under cw operation of a storage ring FEL, an equilibrium of the energy spread is found, balancing the laser induced heating and the damping due to synchrotron motion. When the FEL is implemented on a storage ring, an optical klystron is generally used [3] in order to artificially increase the gain due to the limited straight section length. It consists of two identical undulator separated by a dispersive section, creating a large wiggle of magnetic field allowing the radiation of the two undulators to interfere and the FEL gain to be enhanced. The modulation rate (i.e. the contrast of the fringes) leads to an additional term in the gain relationship, as [4]:

$$f_{\text{mod}} = \exp[-8\pi(N + N_d)^2 \left(\frac{\sigma_\gamma}{\gamma}\right)^2] \quad (1)$$

where N , N_d and σ_γ/γ are the period of undulator,

the number of wavelength passing over an electron in a dispersive section and the relative energy spread, respectively.

Because of its exponential dependence with the energy spread, the modulation rate then contributes significantly to the gain decrease towards saturation.

The small signal gain can be expressed in a case of a storage ring FEL for planar undulators (Super-ACO case):

$$G_{pl} = 1.12 \times 10^{-13} (N + N_d) K^2 L_{OK}^2 (JJ)^2 f_{\text{mod}} \rho_e F_f / \gamma^3 \quad (2)$$

and for helical undulators (UVSOR-II case):

$$G_{hel} = 1.12 \times 10^{-13} (N + N_d) K^2 L_{OK}^2 f_{\text{mod}} \rho_e F_f / \gamma^3 \quad (3)$$

where K , L_{OK} , ρ_e and (JJ) are the undulator deflecting parameter, the length of an optical klystron, the electron density and the Bessel function factor given by $J_1[K^2/(4+2K^2)] - J_0[K^2/(4+2K^2)]$. F_f representing the transverse overlap between the electron beam and the optical laser field, is the filling factor estimated according to the Colson Elleaume approach [5] which takes into account the wiggling of the electron trajectory under the undulator magnetic field and assumes a Gaussian beam for the light distribution.

A more complex saturation process can take place when some coupling between longitudinal and transverse dynamics is introduced, as for instance, by setting the optical klystron in a non dispersive free straight section.

STORAGE RING CHROMATIC OPERATING POINTS

The new trend of the third generation synchrotron light source tends to distribute dispersive function along the straight sections, in order to further reduce the electron beam emittance and increase the brilliance of the photon beam. First investigations have been performed on Super-ACO (Orsay, France, shut-down since end of December 2003), aiming at reaching the theoretical minimum emittance [6]. The lattice structure is composed by 8 dipoles and 4 families of quadrupoles with sextupolar corrections. Such a lattice was then slightly adapted for the Free Electron laser operating point, in introducing a more round beam in the FEL interaction region [7], as illustrated in fig. 1. Table 1 compares the beam performances in the two optics, Super-ACO is operated in this case with the 500 MHz harmonic cavity tuned to the passive mode for an easier setting of the achromatic operating point. In this case, there is also a change of the momentum compaction factor, which may make more complex the understanding of the FEL interaction and saturation process.

*work supported by the Joint Studies Program (2003-2005) of the Institute for Molecular Science

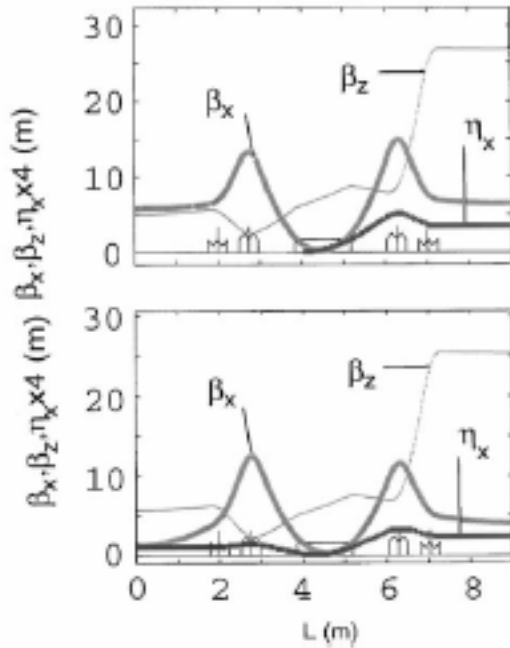


Figure 1: Super-ACO fourth cell beam optics with nominal and reduced α

Table 1: Main Super-ACO storage ring characteristics: beam energy 800 MeV, revolution period 240 ns, 100 MHz RF cavity voltage 170 KV. Horizontal and vertical tunes ν_x and ν_y . Beam transverse dimension (σ_x, σ_y) at the center of the optical klystron.

| | | |
|---|---------------------|---------------------|
| α | 0.0148 | 0.008 |
| $\varepsilon_x, \varepsilon_y$ (nmrad) | 18, 18 | 6.3, 6.3 |
| β_x, β_y (m) betatron functions | 5.4, 5.4 | 1.2, 5.8 |
| η_x (m) | 0 | 0.26 |
| ν_x, ν_y tunes | 4.720, 1.698 | 5.781, 1.768 |
| σ_x, σ_y (μm) | 389, 387 | 165, 191 |
| f_s (kHz) | 14.3 | 10.5 |
| σ_τ (ps) (theor.) | 85 | 62 |
| $\sigma\gamma/\gamma$ (theor.) | $5.4 \cdot 10^{-4}$ | $5.4 \cdot 10^{-4}$ |

On the UVSOR storage ring, the magnetic lattice was reconstructed in 2003 and all the quadrupole magnets and beam ducts are replaced to new ones. With the new optical lattice configuration, the beam emittance was reduced to 1/6 of the previous value [8]. In a usual operation, the chromatic optics is employed. The storage ring can be also operated in a achromatic optics without changing betatron tunes and momentum compaction

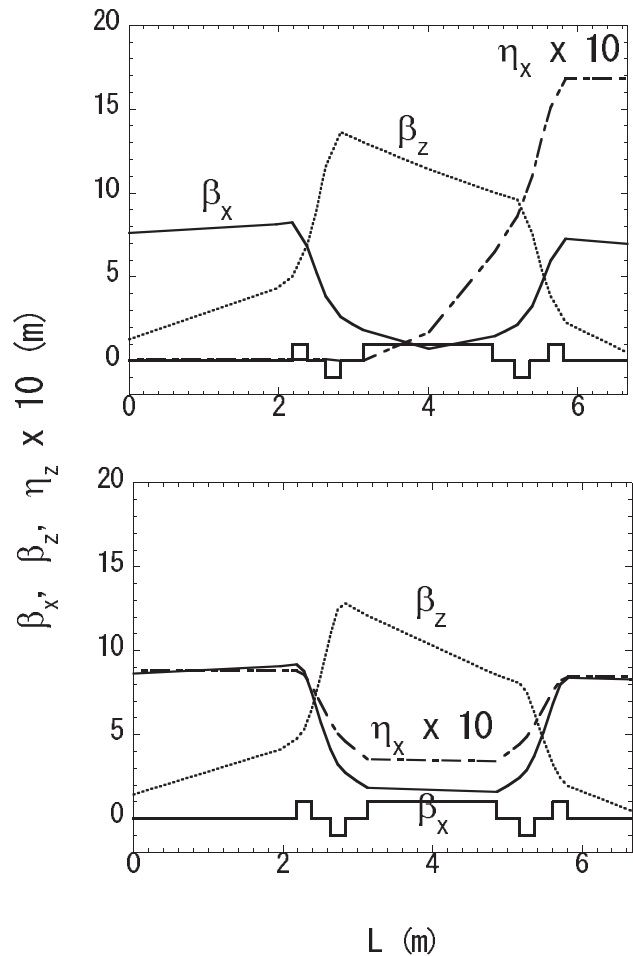


Figure 2: UVSOR-II fourth cell beam optics with the achromatic and the chromatic lattice, in the case of the FEL operation point at 600 MeV. The optical klystron is placed in the center of the long straight section ($L=0$ m)

Table 2: Main UVSOR-II storage ring characteristics: beam energy 600 MeV, revolution period 177.6 ns, 90 MHz RF cavity voltage 55 KV. Horizontal and vertical tunes ν_x and ν_y . Beam transverse dimension (σ_x, σ_y) at the center of the optical klystron.

| | | |
|---|---------------------|---------------------|
| α | 0.026 | 0.026 |
| $\varepsilon_x, \varepsilon_y$ (nmrad) | 45.2, 3 | 18, 0.9 |
| β_x, β_y (m) betatron functions | 7.6, 1.3 | 8.6, 1.4 |
| η_x (m) | 0 (achromatic) | 0.8 (chromatic) |
| ν_x, ν_y tunes | 3.75, 3.20 | 3.75, 3.20 |
| σ_x, σ_y (μm) | 580, 54 | 460, 35 |
| f_s (kHz) | 14.4 | 14.4 |
| σ_τ (ps) (theor.) | 105 | 105 |
| $\sigma\gamma/\gamma$ (theor.) | $3.4 \cdot 10^{-4}$ | $3.4 \cdot 10^{-4}$ |

factor. In this case the emittance is increased by factor of 2.5. Detailed parameters are shown in table 2.

The characteristics of the Super-ACO and UVSOR-II FELs are reported in Table III. The UVSOR-II FEL operates with planar to helical adjustable undulators, and the helical configuration was selected for the present analysis.

Table 3: Main FEL characteristics on Super-ACO and UVSOR-II for the measurements

| | | Super-ACO | UVSOR II |
|----------------------------|----|-----------|----------|
| Optical cavity length | m | 18 | 13.3 |
| circumference | m | 72 | 53.3 |
| Number of stored bunches | | 2 | 2 |
| Undulator | | | |
| deflection parameter K | | 4.96 | 3.47 |
| spatial period λ_0 | cm | 12.9 | 11.0 |
| Number of periods | | 10 | 9 |
| Type | | Planar | Helical |
| Fundamental wavelength | nm | 350 | 520 |
| Cavity losses | % | 0.9 | 0.3 |

In both cases, the longitudinal electron beam distribution is characterised with a double sweep streak camera (Hamamatsu 5680). In the Super-ACO case (see fig. 3), a bunch length reduction is observed for low values of the ring current, because the reduction of the momentum compaction factor. The observed bunch lengthening is mainly due to the microwave instability (threshold of 10 mA/bunch), with a ring impedance of the order of 4 Ω [9].

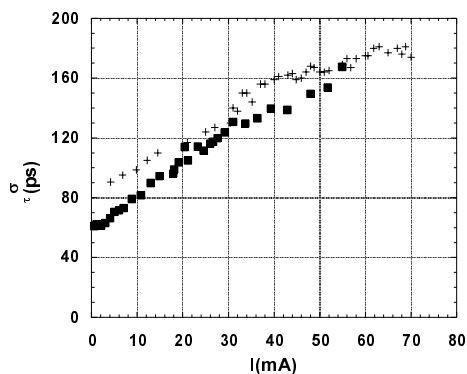


Figure 3: Super-ACO bunch length (σ_τ) versus current for nominal (+) and low α .

In the UVSOR II case, no change of the bunch length is observed between the chromatic and the achromatic points. Here, the bunch distribution evolves up to 100 mA/bunches in the regime of potential well distortion, and the threshold of microwave instability has been determined to be at 70 mA/bunch [10] for an impedance of 4.2 Ω . Both cases, the longitudinal electron beam distribution is characterised with a double sweep streak camera.

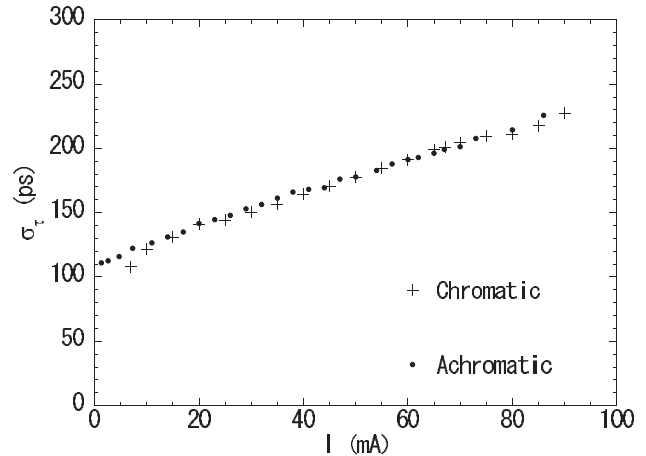


Figure 4: Bunch length versus current in the UVSOR-II case.

Besides, the energy spread has been measured either in analysing the modulation rate of the optical klystron, or by deducing from the transverse beam profile in a non dispersion free location. The energy spread dependence versus the current for Super-ACO is shown in fig. 5 and for UVSOR-II in fig. 6. The potential well distortion regime in which the energy spread remains roughly constant is much smaller in the Super-ACO case (up to 20 mA) than in the UVSOR-II case (up to 140 mA), thanks to a particular care devoted to the vacuum chambers during the up-grade. Quasi zero current values are found in good agreement with theoretical expectations in both cases. In the Super-ACO case, the energy spread enhancement due to microwave instability is larger for the low emittance optics.

The transverse sizes are measured using beam profile monitors. The measured electron bunch dimensions are then introduced in the gain relationship, as shown in figure 7 for Super-ACO and figure 8 for UVSOR-II. The gain increase in the Super-ACO case is mainly due to the smaller values of the beam transverse dimensions at the optical klystron location, with rather similar values in both planes, leading to a good optimisation of the Filling Factor. In the UVSOR-II case, one also observes as well an increase of the gain for the chromatic optics, due to the reduction of the emittance. In this case, there is a difference between the horizontal and vertical sizes, leading to a low value of the filling factor. Nevertheless,

the gain is slightly higher than in the Super-ACO nominal case, thanks to the helical configuration of the undulators, and to a slightly smaller electron beam energy.

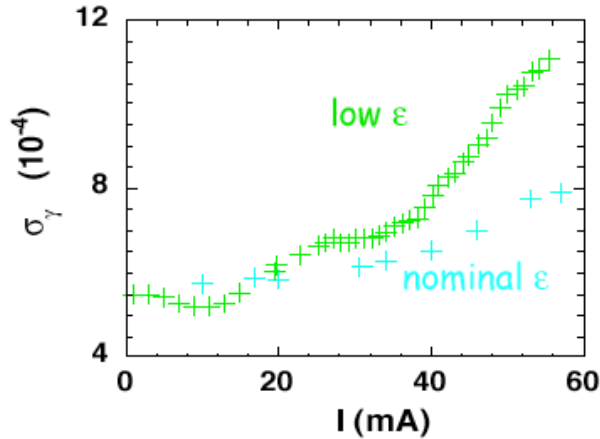


Figure 5: Energy spread versus current in the Super-ACO case without FEL for the two operating points

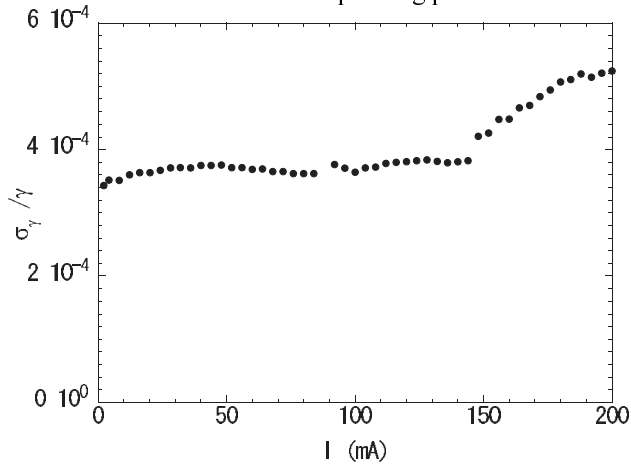


Figure 6: Energy spread versus current in the UVSOR-II case, without FEL. Two electron bunches are stored.

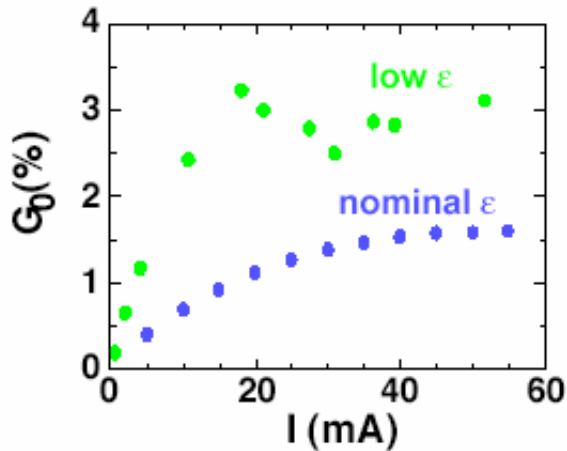


Figure 7: FEL gain in the Super-ACO case

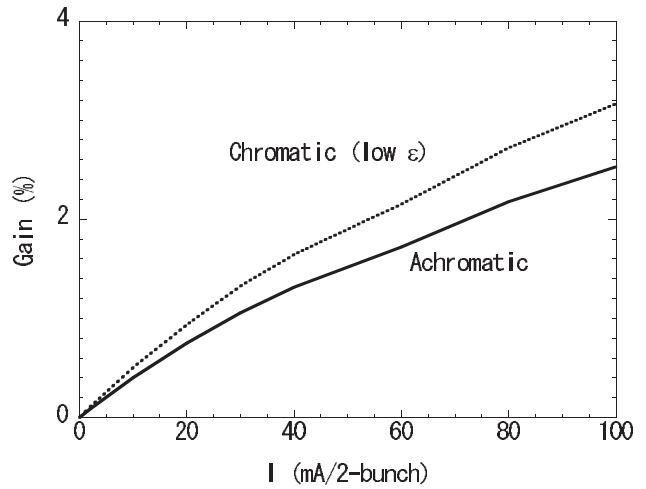


Figure 8: FEL gain in the UVSOR II case

ELECTRON BUNCH HEATING INDUCED BY THE FEL FOR ACHROMATIC AND CHROMATIC OPERATING POINTS

The interaction between the FEL and the electron bunch leads to an energy exchange and the optical wave is amplified to the detriment of the kinetic energy of the relativistic electron. The energy exchange and the laser growth induced to an increase of energy spread of the electron beam, and to FEL saturation. The energy spread can no more be measured directly using the optical klystron spectrum since the FEL light has grown from this spontaneous emission spectrum. The energy spread modification due to the FEL can still be deduced from the electron beam profile measurement performed in a dispersive location. Further measurements on the bunch length can be done using the double sweep streak camera.

In the Super-ACO case, the electron bunch heating in the achromatic point is rather small, as shown in fig. 9a. In fact, the FEL competes with the phenomena responsible of the microwave instability, and can significantly damp it, depending on the gain to cavity losses ratio [11]. In such a case, the electron bunch heating should be compared to the zero current value. Practically no change of the energy spread has been observed in the chromatic mode of operation, as illustrated in figure 9b.

In the UVSOR-II case, the measurements are performed mainly in a current region where the potential well distortion dominates, which makes much more clear the heating induced by the FEL in absence of competition with microwave instability. The FEL induced bunch lengthening has been measured for both optics (see fig. 10) and a smaller heating is observed in the chromatic case.

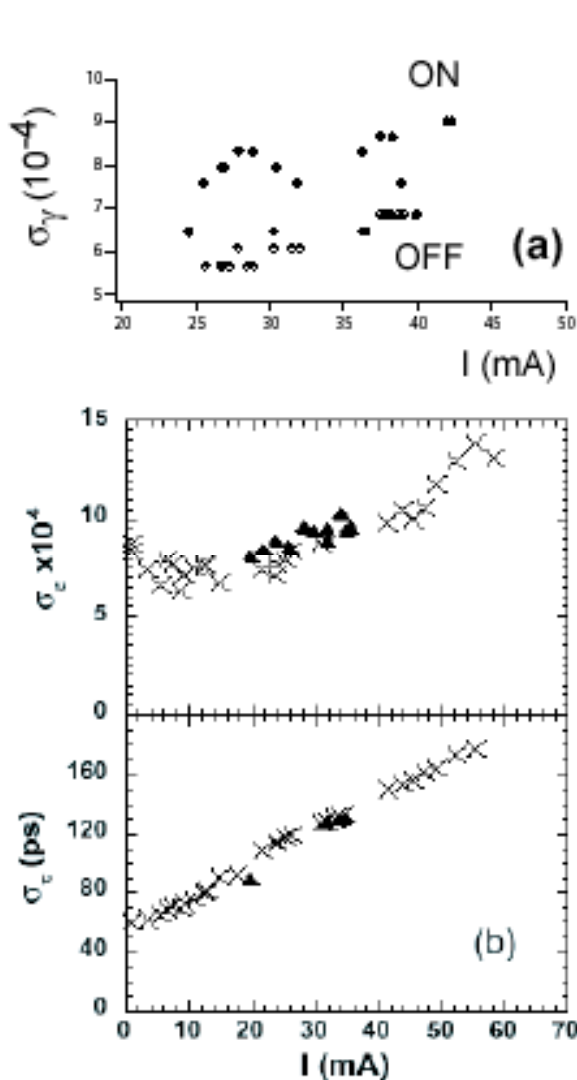


Figure 9: a) FEL induced energy spread heating in the achromatic operating point of Super-ACO. b) Electron bunch heating in the Super-ACO case. Energy spread and bunch length. Triangles : chromatic point. Crosses: Achromatic point.

Besides, when dispersion is introduced at the straight section where the optical klystron is implemented, the FEL induced energy spread leads to an increase of the horizontal size of the electron bunch, as illustrated in fig. 11a for Super-ACO and in fig. 11b for UVSOR-II. In contrast, in the case of the achromatic optics, no change of the transverse sizes has been measured, both on Super-ACO and UVSOR-II. The vertical size is also increased due to the FEL, in particular in the case of Super-ACO where the machine has been set on a coupling resonance for a better optimisation of the filling factor. In the UVSOR-II case, the coupling is expected to be small ($\sim 5\%$) as compared in the case of Super-ACO, however the vertical size is increased more than factor of 3 at 100 mA. Such a change of the electronic density is accompanied by an increase of the Touschek lifetime. A factor of 2 is

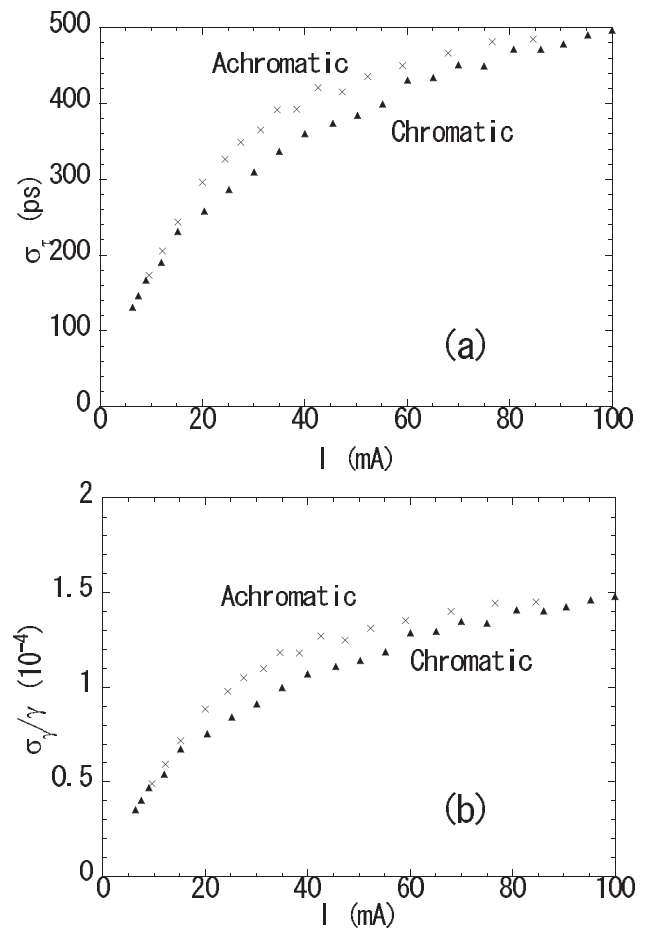
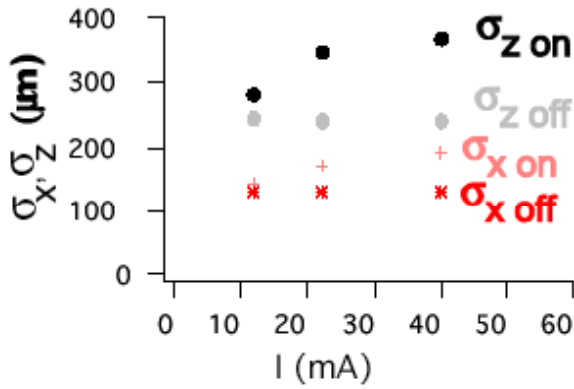


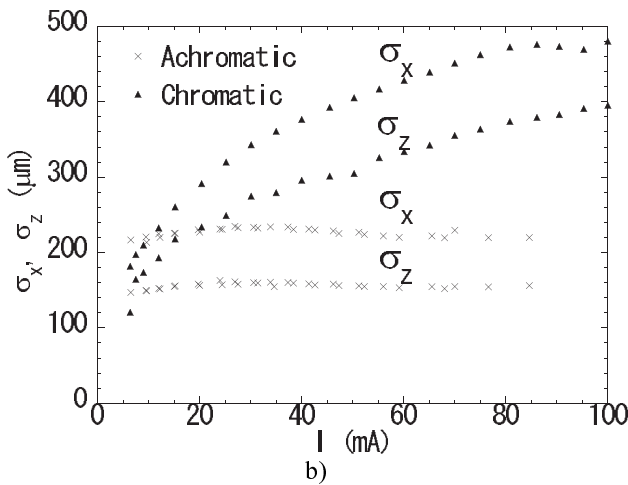
Figure 10: FEL induced bunch lengthening observed in the UVSOR-II case : achromatic and chromatic operating points. a) Heated bunch length and b) energy spread deduced from the bunch lengthening assuming Haissinski model with a inductive impedance of 70nH.

measured at Super-ACO for 40 mA, and more than 20 for UVSOR-II.

The increase of the transverse size leads to a further decrease of the electronic density, and contributes to the gain reduction towards saturation. In addition, the modification of the transverse dimensions of the electron beam induces a change of the filling factor, and a further gain reduction. As a consequence, for an equivalent gain to cavity losses ratio, a smaller induced energy spread is required to reach saturation. In fact, the operating point for the chromatic optics leads also to a slightly higher gain. Finally, the comparison of the induced energy spread for the same cavity losses for the two optics is the result of these two contributions. Nevertheless, slightly smaller energy spread enhancements can be observed in both cases for the chromatic operating point, as presented in fig. 9 and 10. The UVSOR-II case is much more clear than the Super-ACO one, thanks to less changes in the electron beam characteristics (in particular, the momentum compaction factor) and to a much reduced influence of the microwave instability.



a)



b)

Figure 11: Transverse sizes increase due to the FEL in the chromatic operating point. a) Super-ACO b) UVSOR-II

The interplay between the FEL and the electron beam in the chromatic point leads to a more complex saturation process, where the longitudinal and transverse domains can no further be decoupled. The FEL effect on the energy spread is smaller but the FEL modifies also the transverse sizes of the beam. Indeed, the FEL could be considered as a precise tool for modifying the electron beam dynamics.

Such an interpretation is further confirmed by simulations performed with the code LAS, developed in the Orsay [12]. It is based on heuristic equations describing the evolution of the FEL intensity, the gain and the energy spread of the electron beam. It has been modified to include the saturation for the chromatic operating point, by taking into account the gain reduction via the transverse sizes. LAS simulations lead to a smaller energy spread enhancement in the chromatic case with respect to the achromatic one.

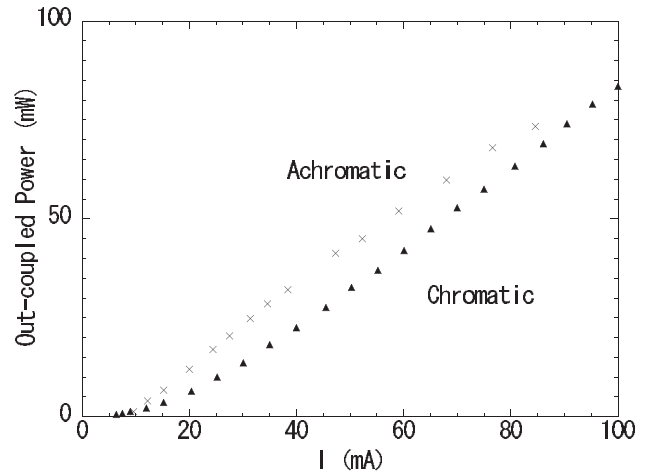


Figure 12: FEL power on UVSOR II for achromatic and chromatic operation.

FEL PERFORMANCES FOR CHROMATIC AND ACHROMATIC OPERATING POINTS

The FEL, power on a storage ring FEL is given by the Renieri limit [13], expressed as follows:

$$8\pi^2\eta_c(N+N_d)f_{\text{mod}}\left(\left(\frac{\sigma_\gamma}{\gamma}\right)_{\text{ON}}^2 - \left(\frac{\sigma_\gamma}{\gamma}\right)_{\text{OFF}}^2\right)P_s \quad (4)$$

with η_c is the ratio between the transmission of the mirror and the total losses of the optical cavity, P_s the synchrotron radiation power, and f_{mod} the modulation factor defined in Eq. (1).

$\left(\frac{\sigma_\gamma}{\gamma}\right)_{\text{ON}}^2 - \left(\frac{\sigma_\gamma}{\gamma}\right)_{\text{OFF}}^2$ correspond to the laser induced energy spread of the beam and the power is directly related to the increase of the energy spread induced by the FEL. In the Super-ACO case, the situation is not very clear and similar FEL power are measured, resulting from the gain increase and the lower necessary energy spread required for the saturation. In the UVSOR-II case, the gain increase being slightly smaller, one sees better a slightly smaller power measured in the case of the chromatic operating point (see fig. 13). The lower FEL power in the chromatic case results as expected from the lower FEL induced energy spread due to the saturation process.

Further analysis can be performed while varying the detuning, i. e. the synchronization between the electron bunch circulating in the ring and the optical pulse bouncing in the optical resonator. The detuning curve usually exhibits five zones. The central region close to the perfect tuning, the FEL is CW and presents the smallest pulse duration and line width. The central zone is surrounded by two zones where the FEL is pulsed, resulting from a limit cycle regime. In the two external

zone, the FEL is again CW, but with a smaller average power and large temporal and spectral distributions of the FEL pulse. When the FEL is detuned, the gain is reduced according to the $\exp(-\tau/2\sigma_\tau)$ with τ the longitudinal position of FEL pulse with respect to the synchronous electron. A reduced increase of energy spread is then necessary to achieve saturation, when the FEL is detune. When the chromatic optics is employed, as a reduced induced FEL heating occurs, the detuning curve widths results to be smaller. This phenomenon has been observed on the UVSOR-II FEL as shown in Fig. 13, and it is well reproduced by the simulations, given in figure 7 of ref [14].

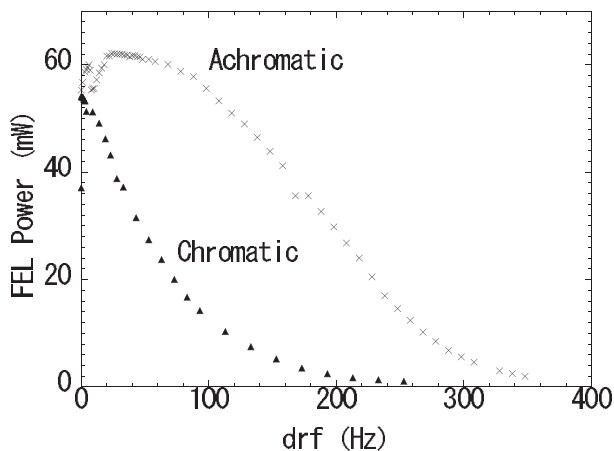


Figure 13: Measured detuning in achromatic and chromatic case. In this experimental, higher reflectivity cavity mirrors of loss value of 0.1 % are employed.

SUMMARY

Electron beam bunch heating process induced by the FEL for the achromatic and chromatic optics was examined in the storage rings Super-ACO and UVSOR-II. Energy spread and transverse size of the electron beam were measured as a function of electron beam. In Super-ACO, no clear difference of induced energy spread for the achromatic and chromatic optics can be observed. The FEL competes with the microwave instability and this obscures the difference in the longitudinal beam characteristics between the two optics. In UVSOR-II, the smaller bunch lengthening in the chromatic case was observed. Whereas, both on SuperACO and UVSOR-II, an increase of the transverse beam size was measured in the chromatic optics, in contrast no change in the achromatic optics. This means that transverse and longitudinal domain is no more decoupled in the chromatics optics. In the UVSOR, the decrease of the electron density contributes to gain reduction and leads less out-coupled power and energy spread.

ACKNOWLEDGEMENTS

The authors would like to thanks C. Bruni, G. L. Orlandi, D. Garzella for their contribution to SuperACO data and S. Bielawski, and S. Swaji for their help on the UVSOR-II experiments. They also like to express their warm thanks to G. Dattoli for faithful discussions.

REFERENCES

- [1] V.N Litvinenko, B. Burnham, J.M.J. Madey, Y. Wu, Nucl.Inst.Meth. A 358, (1995), 334 – 337.
- [2] G.De Ninno, M.E. Couprie, D. Nutarelli, D. Garzella, E. Renault, M.Billardon, Phys. Rev. E64 (2), 6052 (2001).
- [3] NA Vinokurov, AN.Skrinsky, preprint INP77, 59 (1977).
- [4] P. Elleaume, Jour. Physics 40, 5, 373 (1982).
- [5] R. Colson and P. Elleaume Appl. Phys. B29 101 (1982).
- [6] A. Nadji, EPAC 2000 Proceedings, Vienna, Austria. 1057 (2000).
- [7] G. L. Orlandi ,C. Bruni, D. Garzella, M. E. Couprie, G. DeNinno, R. Bartolini, “Super-ACO electron beam dynamics with a reduced compaction factor for Free Electron Laser operation” EPAC 2002, Paris 796 (2002).
C. Bruni et al., Proceedings, FEL 2002, (2003).
- [8] M. Katoh , Synchrotron Radiation News, Vol. 16, No. 6, 33 (2003).
M. Katoh et. al., Nucl. Instru. And Meth. A467-468,68 (2001).
- [9]G. Dattoli, L. Mezi, M. Migliorati, A. Renieri, M. E. Couprie, D. Garzella, D. Nutarelli, C. Thomas, G. DeNinno and R. Walker, Nucl. Inst. and Meth. A471 (2001) 403.
- [10] A. Mochihashi, M. Katoh and M. Hosaka Activity report 2003 36 (2004).
- [11] G. L. Orlandi et al, Phys. Rev. Special Topics-Accelerator and beams 7 (6) No. 060701 (2004).
- [12] M. Billardon, D. Garzella and M. E. Couprie, Phys. Rev. Lett. 69, 2368 (1992).
- [13] D. A. G. Deacon, K. E. Robinson, J. M. J. Madey, C. Bazin, Y. Petroff, M. F. Velghe, M. Billardon, Y. Farge, J. M. Ortega and P. Elleaume, Optics Communications 40 373 (1982).
A. Renieri, Nuovo Ciment B Seri, 53 :160 (1979).
- [14] M. Labat, M. E. Couprie, S. Bielawski, Y. Takashima, M. Hosaka, A. Mochihashi, M. Katoh “ Detuning curve analysis on the UVSOR-II free electron laser “ in this proceedings.